Effects of Inactivating *psbM* and *psbT* on Photodamage and Assembly of Photosystem II in *Synechocystis* sp. PCC 6803[†]

Fiona K. Bentley,[‡] Hao Luo,[‡] Preston Dilbeck,[§] Robert L. Burnap,[§] and Julian J. Eaton-Rye*[,‡]

Department of Biochemistry, University of Otago, Dunedin, New Zealand, and Department of Microbiology and Molecular Genetics, Oklahoma State University, Stillwater, Oklahoma 74078

Received May 4, 2008; Revised Manuscript Received August 28, 2008

ABSTRACT: PsbM and PsbT have been assigned to electron densities on both photosystem II (PSII) monomers at the PSII dimer interface in X-ray crystallographic structures from *Thermosynechoccocus elongatus* and *T. vulcanus*. Our results show that removal of either or both proteins from *Synechocystis* sp. PCC 6803 resulted in photoautotrophic strains but the ΔPsbM:ΔPsbT mutant did not form stable dimers. A CP43-less PSII monomer accumulated in both single mutants, although absence of PsbT destabilized PSII to a greater extent than removing PsbM. Additionally, ΔPsbT cells exhibited slowed electron transfer between the plastoquinone electron acceptors, Q_A and Q_B; however, S-state cycling in both mutants was similar to wild type. Oxygen evolution in these mutants rapidly inactivated following exposure to high light where recovery required protein synthesis and could proceed in the dark in ΔPsbM cells but required light in ΔPsbT cells. Interestingly, the extent of recovery of oxygen-evolving activity was greatest in the ΔPsbM:ΔPsbT strain. We also found recovery required Psb27 in ΔPsbT cells although, under our conditions, the ΔPsb27 strain remained similar to wild type. In contrast, the ΔPsbM:ΔPsb27 mutant could not assemble PSII beyond a CP43-minus intermediate. Our results suggest essential roles for Psb27 in biogenesis in the ΔPsbM strain and for repair from photodamage in cells lacking PsbT.

The mesophilic cyanobacterium *Synechocystis* sp. PCC[1] 6803 has been widely used as a model organism for the study of photosystem II (PSII) of oxygenic photosynthesis (*1*−*3*). In addition, the stability of PSII preparations from two thermophilic species, *Thermosynechococcus elongatus* and *T. vulcanus*, has resulted in X-ray crystallographic structures of oxygen-evolving PSII dimeric complexes at resolutions of 3.0−3.4 Å (*4*−*6*). However, the physiological significance of PSII dimer formation has not been established and biochemical studies with these organisms have identified both monomeric and dimeric forms (*7, 8*) with each monomer known to comprise at least 20 protein subunits (*9*).

X-ray-derived structures of PSII place three low-molecular-weight polypeptides: PsbL, PsbM and PsbT—each containing a single membrane-spanning α helix—at the monomer−monomer interface (*4*−*6*). The two copies of PsbM are found adjacent to each other and are flanked by PsbL and PsbT with each monomer contributing a copy of each polypeptide (*4, 5*). PsbL is ∼4.5 kDa and highly conserved among plants, algae and cyanobacteria, particularly in the membrane-spanning C-terminal half of the polypeptide (Figure S1 in the Supporting Information). In *Synechocystis* sp. PCC 6803, PsbM is ∼3.9 kDa with considerable similarity to other PsbM sequences from cyanobacteria (Figure S2 in the Supporting Information). However, more variation is found with this polypeptide than either PsbL or PsbT and strains of *Prochlorococcus marinus* possess a C-terminal extension of ∼18 residues of unknown function. The PsbT protein (Figure S3 in the Supporting Information) is ∼3.5 kDa, and both PsbM and PsbT have their C-termini located on the cytosolic side of the thylakoid membrane.

The gene encoding PsbL is found in the *psbEFLJ* operon, and deletion of *psbL* in *Synechocystis* sp. PCC 6803 resulted in an obligate photoheterotrophic strain that lacked PSII oxygen-evolving activity (*10*). To date, the effect of inactivating *psbM* in cyanobacteria has not been reported; however, the *psbT* gene has been disrupted in *T. elongatus* and diminished levels of dimeric PSII and reduced levels of PsbM were observed (*7*). Despite this phenotype, the oxygen-evolving activity of cells, isolated thylakoids and isolated PSII complexes was found to be similar between the ΔPsbT mutant and wild type: moreover, photoautotrophic growth of ΔPsbT and wild-type cells did not differ across a wide range of light intensities. In contrast, a ΔPsbT strain of the green alga *Chlamydomonas reinhardtii* was found to be impaired in recovery of PSII following photodamage and to have both a reduced affinity for the primary plastoquinone

[†] This work was supported by a grant (UOO309) from the New Zealand Marsden Fund to J.J.E.-R.

* To whom correspondence should be addressed. Tel: 64 3 479-7865. Fax: 64 3 479-7866. E-mail: julian.eaton-rye@stonebow.otago.ac.nz.

[‡] University of Otago.

[§] Oklahoma State University.

[1] Abbreviations: BN−PAGE, blue-native polyacrylamide gel electrophoresis; bp, base pairs; DCMU, 3-(3,4-dichlorophenyl)-1,1-dimethylurea; DMBQ, 2,5-dimethyl-*p*-benzoquinone; HEPES, 4-(2-hydroxyethyl)-1-piperazineethanesulfonic acid; kb, kilobases; nt, nucleotides; OD, optical density; OEC, oxygen-evolving complex; ORF, open reading frame; PCC, Pasteur Culture Collection; PCR, polymerase chain reaction; PVDF, polyvinylidene fluoride; PQ, plastoquinone; PSI, photosystem I; PSII, photosystem II; Q_A, primary quinone electron acceptor of photosystem II; Q_B, secondary quinone electron acceptor of photosystem II; SDS, sodium dodecyl sulfate; TES, 2-[tris(hydroxymethyl)methyl]amino-1-ethanesulfonic acid.

10.1021/bi800804h CCC: $40.75 © 2008 American Chemical Society
Published on Web 10/04/2008

electron acceptor, Q_A, and impaired photoreduction of Q_A (*11, 12*).

In this study we have constructed ΔPsbM and ΔPsbT strains of *Synechocystis* sp. PCC 6803 to establish the relative importance of these polypeptides in PSII activity under optimal and photoinhibitory conditions. Oxygen evolution was impaired in both of these mutants and rapidly inactivated under high light. In addition, oxidation of Q_A^- was retarded in ΔPsbT cells: and even though both ΔPsbM and ΔPsbT strains remained photoautotrophic, they accumulated CP43-less inactive PSII monomers. We also created a ΔPsbL strain in which only CP43-less monomers could be detected although it retained a limited capacity for photoautotrophic growth. In addition, the ΔPsbM:ΔPsbT double mutant was found to only contain monomeric forms of PSII but remained photoautotrophic. Finally, recovery of photodamaged PSII, in ΔPsbT cells, required the extrinsic Psb27 protein; whereas PSII did not assemble beyond the CP43-less inactive monomer if Psb27 was absent in the ΔPsbM mutant. These findings therefore establish unique roles for PsbM and PsbT in cyanobacterial PSII and provide new information regarding the requirement for PsbL in *Synechocystis* sp. PCC 6803. In addition, our results suggest a role for Psb27 in both PSII biogenesis and repair.

MATERIALS AND METHODS

Growth of Synechocystis sp. PCC 6803 Strains. Cultures were maintained on solid BG-11 media containing 5 mM glucose, 20 μM atrazine, 10 mM TES-NaOH (pH 8.2), 0.3% sodium thiosulfate and appropriate antibiotics (*13*). Liquid cultures were grown mixotrophically in unbuffered BG-11 media containing 5 mM glucose and appropriate antibiotics. In both solid and liquid media erythromycin and spectinomycin were present at a concentration of 25 μg/mL and chloramphenicol at a concentration of 15 μg/mL. Cultures were maintained at 30 °C under constant illumination at 30 μE m^{-2} s^{-1}. Photoautotrophic growth experiments were carried out as described in refs *13* and *14*. The *Synechocystis* sp. PCC 6803 strain used in this study was the glucose-tolerant strain described in ref *1*, and this is referred to throughout as wild type.

Construction of Synechocystis sp. PCC 6803 Mutant Strains. The open-reading frames (ORFs) smr0007, sml0003, smr0001 and slr1645, which encode the *psbL*, *psbM*, *psbT* and *psb27* genes, respectively, were obtained by PCR: smr0007 was amplified using the forward primer 5′-TGGCCGTTATGTGGCGGTGTCAGCC-3′ and reverse primer 5′-AGTGGGCCAAGCCCACCTTAAAACC-3′; sml0003 was amplified using the forward primer 5′-CAGGGGGACGGGCCAACACAAACAC-3′ and reverse primer 5′-CGGCGGTGCAAAAGGCATCGATCAC-3′; smr0001 was amplified using the forward primer 5′-CGGTTGAGCATTGACCCGATGGCTG-3′ and reverse primer 5′-TTCGTGATGACGGTAACCTCTGCCG-3′, and slr1645 was amplified using the forward primer 5′-AAGACCCAACTGGAGGACAATGCGG-3′ and reverse primer 5′-CAATGCCTCTAGGGCTGCCTGTTT G-3′. The cloned *psbL* gene was interrupted at a unique intragenic *Van*91I site by a chloramphenicol-resistance cassette derived from pBR325 (*15, 16*). Most of the *psbM* coding sequence was deleted using *Hpa*I sites within and flanking the *psbM* gene, and replaced with an erythromycin-resistance cassette derived from pRL425 (*17*). The cloned *psbT* gene was interrupted at a unique intragenic *Nco*I site by a spectinomycin-resistance cassette derived from pHP45Ω (*18*). The cloned *psb27* gene was interrupted at a unique intragenic *Cla*I site by the chloramphenicol-resistance cassette derived from pBR325. The interrupted genes were then used to transform *Synechocystis* sp. PCC 6803 according to established protocols (*1, 13*). Complete segregation for the introduced antibiotic-resistance cassettes was verified by PCR using the appropriate forward and reverse primers described above.

Measurement of the Relative Level of Assembled PSII Centers. Herbicide-binding assays measuring 3-(3,4-dichlorophenyl)-1,1-dimethylurea (DCMU)-replaceable [^{14}C]atrazine binding were used to estimate the relative level of assembled PSII centers on a chlorophyll basis (*19, 20*). The specific activity of the [^{14}C]atrazine was 17.1 mCi/mmol.

Oxygen Evolution and Photoinactivation Assays. Cells were grown in BG-11 containing 5 mM glucose before being harvested. Following removal of glucose, cells were maintained at 30 °C in BG-11 containing 25 mM HEPES-NaOH, pH 7.5, at a chlorophyll concentration of 10 μg/mL. Oxygen evolution was measured with a Clark-type electrode (Hansatech, King's Lynn, U.K.) at 30 °C using 3.0 mM $K_3Fe(CN)_6$ and 0.6 mM 2,5-dimethyl-*p*-benzoquinone (DMBQ) as electron acceptors. Saturating actinic light (2 mE m^{-2} s^{-1}) was provided by an FLS1 light source (Hansatech, King's Lynn, U.K.) passed through a Melis Griot OG 590 sharp cutoff red glass filter. Photoinactivation was achieved using 2 mE m^{-2} s^{-1} white light from a Kodak Ektalite 1000 slide projector. When added, chloramphenicol was at a concentration of 250 μg/mL.

Decay Kinetics of Chlorophyll a Fluorescence. Measurements of the decay kinetics of chlorophyll fluorescence were performed with a double modulation kinetic fluorometer (PSI Instruments, Brno, Czech Republic). Cells in liquid culture were harvested at midlogarithmic growth phase by centrifugation at 4000*g* for 5 min at room temperature, resuspended in BG-11 to a chlorophyll concentration of 80 μg/mL and incubated on a shaker at 200 rpm under dim light at room temperature for 30 min before being diluted to a chlorophyll concentration of 4 μg/mL for measurements. The low fluorescence F_0 state in dark-adapted samples was measured by a series of four measuring pulses. This was followed 200 μs later by a 30 μs saturating actinic flash, and then a sequence of measuring pulses beginning 50 μs after the actinic flash. When added, DCMU was at a final concentration of 20 μM.

Flash Oxygen Yield Measurements. Cells in liquid culture were harvested at mid-logarithmic growth phase by centrifugation at 4000*g* for 5 min at room temperature, resuspended in BG-11 to a chlorophyll concentration of 80 μg/mL and incubated on a shaker at 200 rpm under dim light at room temperature for 30 min. For measurements, cells were diluted to 8 μg/mL in 10 mM HEPES-NaOH (pH 7.1) and 30 mM NaCl. Oxygen evolution was determined polarographically using a centrifugal bare platinum electrode described in (*21*). Cells were centrifugally deposited onto the platinum surface of the electrode at 18000*g* for 5 min in a Sorvall HB-4A swing-out rotor. Flash-induced oxygen yields of dark-adapted cells were measured during a series of saturating xenon flashes at 4 Hz. To measure the decay

kinetics of the S_2 state, PSII centers were advanced to the S_2 state by an initial single saturating flash. The lifetime of the S_2 state was measured through a subsequent series of saturating flashes given at 10 s, 20 s, 40 s, 60 s, 120 s, 240 or 480 s after the initial flash, and recording the amplitude of the oxygen yield on the third flash. Cells were dark adapted for 10 min between each measurement.

Thylakoid Isolation. Synechocystis sp. PCC 6803 cells were harvested and resuspended in isolation buffer (50 mM HEPES−NaOH (pH 7.2), 10 mM $MgCl_2$, 5 mM $CaCl_2$ and 1 M sucrose) together with protease inhibitors (1 mM ε-caproic acid, 1 mM phenylmethylsulfonyl fluoride, and 2 mM benzamidine) and broken by glass beads (0.1 mm diameter) at 5 000 rpm using a Mini-Beadbeater (BioSpec Products, Inc., Bartlesville, OK). Five 20 s cycles were performed with a 5 min incubation on ice between each iteration. Beads were removed by centrifugation at 900*g* for 5 min. Thylakoids were then pelleted by centrifugation at 200000*g* for 30 min at 4 °C, and finally resuspended in isolation buffer with protease inhibitors and stored in liquid nitrogen for later use in blue-native polyacrylamide gel electrophoresis (BN−PAGE). Chlorophyll concentrations were determined by extraction in 80% acetone as in ref *22*.

Blue-Native PAGE and Immunodetection. Blue-native PAGE was carried out according to ref *23* with modifications to thylakoid solubilization described in ref *24*. Solubilized proteins were loaded on to a 5−12% gradient of acrylamide in the separation gel (gel dimensions: 16 × 16 × 0.1 cm). Electrophoresis was carried out using a Protean II cell (Bio-Rad Laboratories, Hercules, CA) at 4 °C starting at 7 mA for 1 h and continued at 15 mA for 15 h. For immunodetection assays, protein was transferred to PVDF membrane and probed with protein-specific antibodies. Secondary antibodies conjugated to peroxidase allowed detection of native proteins using chemiluminescence (*25*).

Nomenclature of Strains. The different cell lines are referred to by the absence of the specific protein by using the Greek letter Δ (e.g., the ΔPsbM strain etc.) without distinguishing if this arose from deletion of the corresponding gene, as was the case if PsbM was absent, or gene interruption, as was used to remove PsbL and PsbT. To indicate the absence of more than one protein, as for example in the double mutant, ΔPsbM:ΔPsbT, the two deletions have been separated by a colon.

RESULTS

Effects of Removing PsbL, PsbM and PsbT on Photoautotrophy and Assembly of PSII. To identify specific roles for PsbM and PsbT in *Synechocystis* sp. PCC 6803, we assembled strains lacking functional copies of their respective genes: and, for comparison, a ΔPsbL strain was also constructed (cf. ref *10*.). Gene cassettes conferring resistance to spectinomycin and chloramphenicol were inserted into the coding regions of *psbL* and *psbT,* respectively, and the ORF of *psbM* replaced by an erythromycin-resistance cassette. Complete segregation of the inactivated genes was verified by PCR (Figure 1).

Requirements for these polypeptides were initially examined by measuring photoautotrophic growth (Figure 2A). Wild type had a doubling time of 14 h, whereas the ΔPsbM and ΔPsbT strains exhibited doubling times of 24 and 18 h,

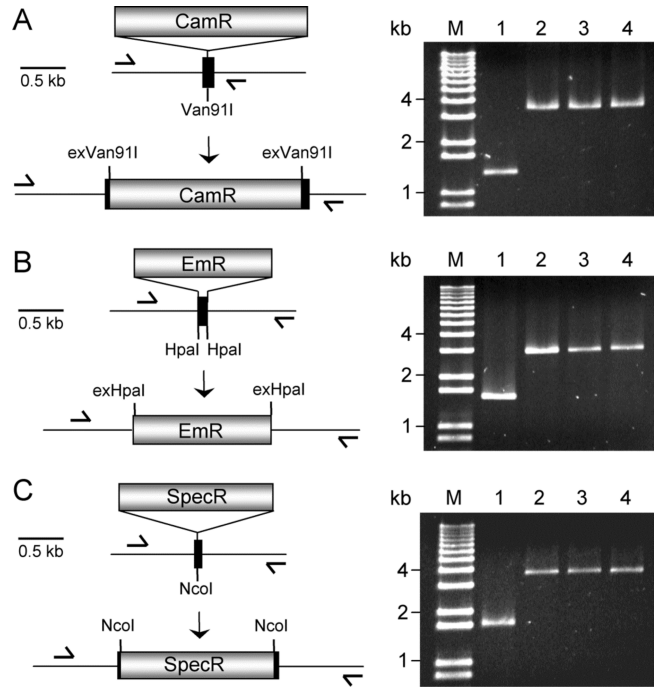

FIGURE 1: Construction of *Synechocystis* sp. PCC 6803 mutant strains. (A) Insertion of a 2.0-kb chloramphenicol-resistance cassette (CamR) at the unique intragenic *Van*91I site of *psbL*. PCR confirmed the complete replacement of *psbL* with the interrupted gene. The primers used in the reaction are indicated with arrows, and the PCR products from different strains are shown on the gel. Lanes: M, 1 Kb Plus DNA Ladder (Invitrogen Carlsbad, CA); 1, wild type; 2, ΔPsbL; 3, ΔPsbL:ΔPsbM; 4, ΔPsbL:ΔPsbT. (B) Deletion of *psbM* between two *Hpa*I sites and replacement with a 1.5-kb erythromycin-resistance cassette (EmR). PCR confirmed replacement of *psbM*. The PCR products from different strains are shown. Lanes: M, 1 Kb Plus DNA Ladder (Invitrogen, Carlsbad, CA); 1, wild type; 2, ΔPsbM; 3, ΔPsbL:ΔPsbM; 4, ΔPsbM:ΔPsbT. (C) Insertion of a 2.0-kb spectinomycin-resistance cassette (SpecR) at the unique intragenic *Nco*I site of *psbT*. PCR confirmed complete replacement of *psbT* with the interrupted gene. The PCR products from different strains are shown. Lanes: M, 1 Kb Plus DNA Ladder (Invitrogen Carlsbad, CA); 1, wild type; 2, ΔPsbT; 3, ΔPsbL:ΔPsbT; 4, ΔPsbM:ΔPsbT.

respectively. In contrast, removal of PsbL extended this to >120 h. Moreover, limited growth of ΔPsbL cells was abolished in the ΔPsbL:ΔPsbM and ΔPsbL:ΔPsbT mutants. However, the ΔPsbM:ΔPsbT strain remained photoautotrophic with a doubling time of 26 h (Figure 2B).

Oxygen evolution, supported by $K_3Fe(CN)_6$ and DMBQ, was measured to assess PSII-specific activity. In Figure 2C, the ΔPsbM and ΔPsbT mutants had oxygen-evolving rates of 78% and 62%, respectively, when compared to wild type. Removal of both PsbM and PsbT in the ΔPsbM:ΔPsbT strain had an additive effect, with oxygen evolution reduced to 33%. Additionally, oxygen evolution from the ΔPsbM, ΔPsbT and ΔPsbM:ΔPsbT strains showed a gradual decline over the 3 min illumination period, indicative of photoinactivation of PSII. In contrast, wild type evolved oxygen at a relatively constant rate during the exposure to actinic light. However, under the assay conditions, neither the ΔPsbL strain nor the ΔPsbL:ΔPsbM and ΔPsbL:ΔPsbT mutants exhibited measurable levels of oxygen evolution.

To assess PSII assembly, DCMU-replaceable [^{14}C]atrazine binding was performed in whole cells. These data (Figure 2D) indicate that the ΔPsbM and ΔPsbT strains were capable of assembling PSII at 72% and 40%,

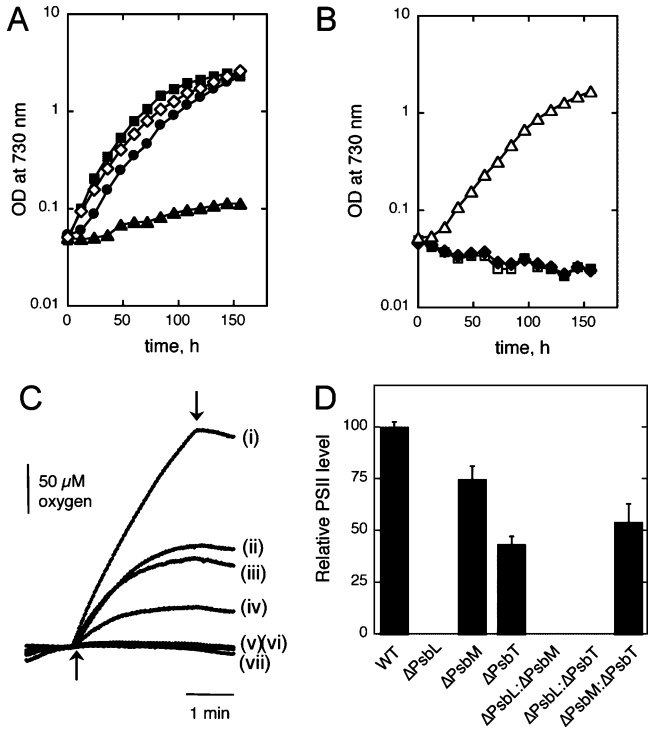

FIGURE 2: Characterization of *Synechocystis* sp. PCC 6803 mutant strains. (A) Photoautotrophic growth of single mutants in BG-11 media as measured by optical density at 730 nm. Strains shown are wild type (closed squares), ΔPsbL (closed triangles), ΔPsbM (closed circles), and ΔPsbT (open diamonds). Data are representative of three independent experiments. (B) Photoautotrophic growth of double mutants. Strains shown are ΔPsbL:ΔPsbM (open squares), ΔPsbL:ΔPsbT (closed diamonds), and ΔPsbM:ΔPsbT (open triangles). Data are representative of three independent experiments. (C) Traces of oxygen evolution determined polarographically in the presence of $K_3Fe(CN)_6$ and DMBQ. The 1 mL reaction chamber held cell suspensions containing 10 μg of chlorophyll/mL. Average initial rates of oxygen evolution over the first min of illumination are given in μmol of O_2 (mg of chlorophyll)$^{-1}$ h^{-1}. Data are representative of three independent experiments, and rates were reproducible to within 15% of the average. (i) Wild type, 483; (ii) ΔPsbM, 377; (iii) ΔPsbT, 300; (iv) ΔPsbM:ΔPsbT, 161; (v) ΔPsbL, no measurable rate; (vi) ΔPsbL:ΔPsbM, no measurable rate; (vii) ΔPsbL:ΔPsbT, no measurable rate. Arrows indicate when light was turned on and off. (D) Relative levels of PSII assembly as determined by DCMU-replaceable [^{14}C]atrazine binding, normalized to a wild-type chlorophyll/PSII ratio of 805. The results are the average ± the standard error of three independent experiments.

respectively, of the level found in wild type: while the ΔPsbM:ΔPsbT mutant assembled 66%. The removal of PsbL in the ΔPsbL, ΔPsbL:ΔPsbM and ΔPsbL:ΔPsbT strains reduced PSII assembly to below the level of detection of this assay which is typically ~20% of the level found in wild-type cells (*20*).

The Effect of Removing PsbM and PsbT on Q_A^- Oxidation in Whole Cells. The decay kinetics of the variable chlorophyll *a* fluorescence yield were measured to assess Q_A^- oxidation. Figure 3 illustrates the normalized decay following a saturating actinic flash in wild type and the ΔPsbM, ΔPsbT and ΔPsbM:ΔPsbT strains. In the absence of DCMU, this decay largely reflects electron transfer from Q_A to Q_B. It is clear that relaxation of the fluorescence yield is quite similar in ΔPsbM and wild-type cells indicating removal of PsbM had little impact upon forward electron transfer. The time (t_{50}) at which the fluorescence decayed to 50% of its initial level was 0.4 ms in wild type and 0.7 ms in the ΔPsbM strain. In contrast, the t_{50} values for the ΔPsbT and ΔPsbM:ΔPsbT strains were 2.2 and 8.2 ms, respectively. These data could be adequately fit assuming three kinetic phases with the two faster phases ascribed to electron transfer between Q_A and Q_B, and a slow phase ascribed to back-reaction with the donor side (Table 1 and ref *26*). In comparison to ΔPsbM and wild-type cells, the ΔPsbT and ΔPsbM:ΔPsbT strains exhibited considerably retarded phases corresponding to forward electron transfer from Q_A to Q_B. The results indicate impaired electron flow between Q_A and Q_B in ΔPsbT cells, which becomes further aggravated upon removal of PsbM. This additional removal of PsbM appears to result in a higher probability of the Q_A^- state recombining with an oxidant on the donor side of the complex as evidenced by the larger amplitude of the slowest phase of fluorescence relaxation in the double mutant (Figure 3 and Table 1).

In contrast to the kinetics in the absence of DCMU, the relaxation of variable chlorophyll *a* fluorescence yield in the presence of DCMU, reflecting recombination of Q_A^- with the S_2 state of the oxygen-evolving complex, was similar for all strains. In wild type the t_{50} for the fluorescence decay was 519 ms. In comparison, the ΔPsbM strain exhibited a t_{50} of 574 ms and the ΔPsbT and ΔPsbM:ΔPsbT strains had t_{50} values of 749 and 674 ms, respectively. These findings suggest a minimal impact upon the redox potential gap between the Q_A/Q_A^- and the S_2/S_1 redox couples. A minimal impact of the mutations upon the oxygen-evolving complex is consistent with the results of the flash-induced oxygen evolution experiments described in the next section and, therefore, the absence of PsbT does not seem to affect the midpoint redox potential of the Q_A/Q_A^- couple. Consequently, the slowed electron transfer from Q_A to Q_B could be due to a downshift in the midpoint potential of Q_B/Q_B^-, decreasing the driving force of electron transfer from Q_A to Q_B, or to alterations in the electron coupling or reorganization energy governing electron transfer between Q_A and Q_B. In either case, it appears that the primary impact of removing PsbT in these cells is upon the acceptor side of the PSII complex.

Flash-Induced Yields of Oxygen Evolution in the ΔPsbM and ΔPsbT Strains. Flash-induced oscillatory patterns of oxygen production were used to assess S-state cycling upon removal of different polypeptides. Figure 4A shows yields for wild type, and the ΔPsbM, ΔPsbT and ΔPsbM:ΔPsbT strains following a sequence of saturating single-turnover flashes at a frequency of 4 Hz. A similar oscillatory pattern was observed for all mutants and was comparable to wild type, indicating a similar distribution of photochemical misses and double hits in all strains (Table S1 in the Supporting Information).

In light of the similar rate of Q_A^- oxidation, in the presence of DCMU, between wild type and mutants (Figure 3) the stability of the S_2 state was investigated. Cells were advanced to the S_2 state by a single saturating flash, and the lifetime of the S_2 state was measured by giving a subsequent series of saturating flashes at varying time intervals after the initial flash and recording the oxygen yield on the third flash. These data were plotted as a function of the time interval between the first and second flashes and represent the kinetics of S_2 decay (Figure 4B). The ΔPsbM and ΔPsbT strains exhibited slightly slower apparent half-times (43 and 37 s, respectively) compared to wild type (32 s). However, these measurements

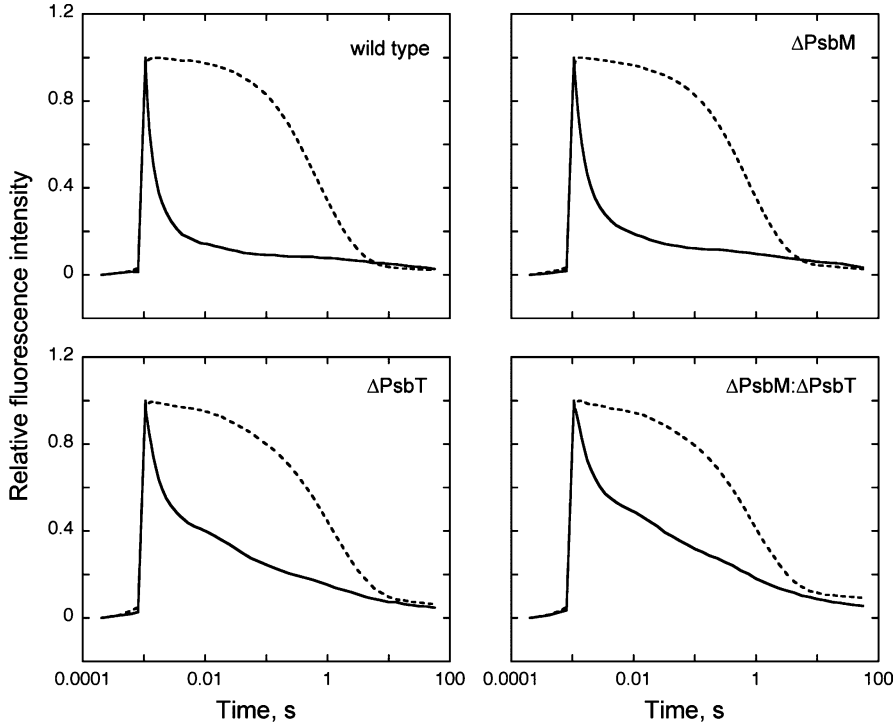

FIGURE 3: Decay of chlorophyll *a* fluorescence yield in whole cells following a single turnover actinic flash in the presence (dashed line) or absence (solid line) of DCMU. The panels are (A) wild type; (B) ΔPsbM; (C) ΔPsbT; and (D) ΔPsbM:ΔPsbT. Cell suspensions contained 4 μg of chlorophyll/mL. Data have been normalized and are the average of three independent experiments.

Table 1: Decay Kinetics of Flash-Induced Variable Fluorescence without DCMU[a]

	fast phase		middle phase		slow phase	
strain	$t_{1/2}$ (μs)	amp (%)	$t_{1/2}$ (ms)	amp (%)	$t_{1/2}$ (s)	amp (%)
wild type	330 ± 20	97 ± 17	4.9 ± 0.5	2 ± 0.1	11.2 ± 2.3	1.0 ± 0.02
ΔPsbM	460 ± 20	95 ± 09	8.8 ± 1.1	3 ± 0.2	10.4 ± 1.7	1.7 ± 0.05
ΔPsbT	1100 ± 80	74 ± 08	61.0 ± 0.1	14 ± 0.4	5.5 ± 0.7	12.0 ± 0.80
ΔPsbM:ΔPsbT	1105 ± 70	70 ± 07	52.2 ± 7.2	16 ± 0.7	3.9 ± 0.5	15.0 ± 0.50

[a] The curves were analyzed in terms of two exponential components (middle and slow phases) and one hyperbolic component (slow phase) according to ref *26*. Standard errors of the calculated parameters are indicated.

suggest the S_2 state is essentially unaltered by the removal of either PsbM or PsbT.

Assembly of PSII Complexes in the ΔPsbM, ΔPsbT and ΔPsbM:ΔPsbT Strains. Blue-native PAGE was used to examine native protein complexes of the thylakoid membrane. Immunodetection, using an antibody against D1, allowed identification of both dimeric and monomeric PSII (Figure 5A). Neither PSII dimers nor monomers were detected in strains lacking PsbL, although the CP43-less assembly intermediate complex was present (cf. Figure 5B and refs *27* and *28*). Moreover, the ΔPsbM, ΔPsbT and ΔPsbM:ΔPsbT strains had elevated levels of the CP43-less monomer (Figure 5A, B). This suggests that progression from the CP43-less subcomplex to the intact PSII monomer is also impaired if either PsbM or PsbT is absent. Even so, PSII dimer bands were present in both the ΔPsbM and ΔPsbT strains, albeit at lower abundance compared to wild type, indicating a sufficient interaction between the two PSII monomers to stabilize the PSII dimer, despite removal of PsbM or PsbT. Additionally, the ΔPsbT strain consistently showed two forms of PSII dimer, apparently differing in molecular weight. Interestingly, no dimers were observed in the ΔPsbM:ΔPsbT strain (Figure 5A, B), hence the combined removal of PsbM and PsbT is sufficient to disrupt the monomer−monomer interaction such that no dimers are detectable using BN−PAGE. Similar results were obtained with antibodies to D2 and CP47 (data not shown).

Effects of Removing PsbM and PsbT on Recovery of PSII Activity Following High-Light Stress. We examined recovery of oxygen-evolving activity in whole cells after 45 min of high-intensity-light stress (2.0 mE m^{-2} s^{-1}) (Figure 6). All strains showed the ability to recover once the stress had been removed (Figure 6A) and, moreover, all strains consistently recovered to exhibit a rate beyond the rate determined before stress was applied. In particular, the ΔPsbM:ΔPsbT mutant reached 170% after 2 h at 0.3 mE m^{-2} s^{-1} (a further 2 h at low light was required before the activity returned to the initial level (data not shown)). Furthermore, addition of chloramphenicol showed the observed recovery was dependent on protein synthesis (Figure 6B).

To investigate the requirement for light in the recovery process oxygen evolution was followed in the dark following high-light exposure (Figure 6C). Both wild type and the ΔPsbM strain exhibited a recovery and stimulation of oxygen evolution following incubation in complete darkness similar to that observed during recovery under 0.3 mE m^{-2} s^{-1} (cf. Figure 6A). In contrast, the ΔPsbT and ΔPsbM:ΔPsbT strains showed a partial recovery, indicating both light-

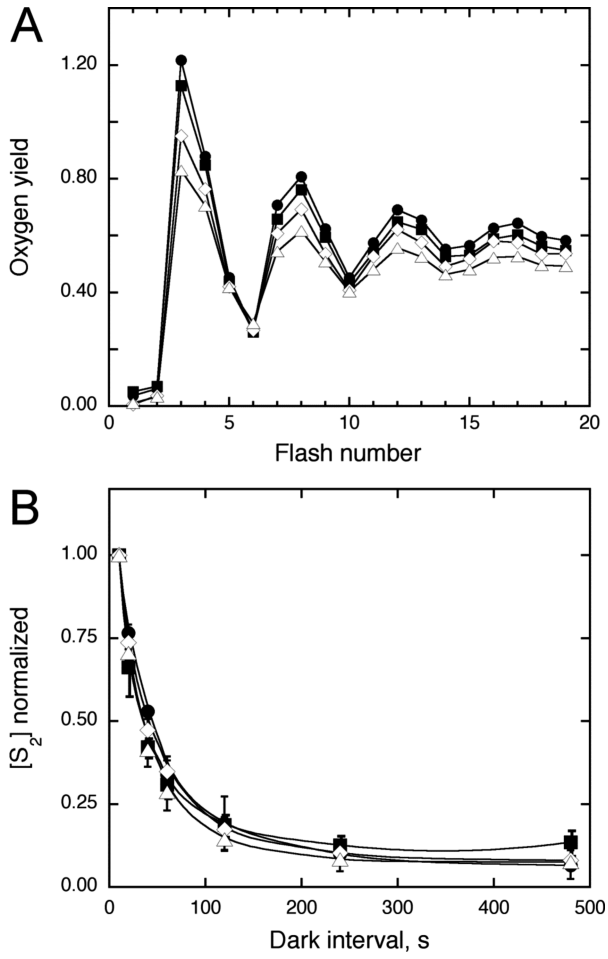

FIGURE 4: (A) Flash-induced oxygen yields in dark-adapted whole cells. Strains shown are: wild type (closed squares), ΔPsbM (closed circles), ΔPsbT (open diamonds), and ΔPsbM:ΔPsbT (open triangles). Data are representative of results obtained in three independent experiments. (B) Decay of the S_2 state in cells of wild type (closed squares), ΔPsbM (closed circles), ΔPsbT (open diamonds), and ΔPsbM:ΔPsbT (open triangles). Measurements of the lifetimes of the S_2-state were performed by recording the amplitude of O_2 yield on the third flash varying the time interval between the first and second flashes. The results are the average ± the standard error of three independent experiments.

dependent and light-independent processes are required for the full restoration of oxygen evolution in these mutants.

The Requirement for Psb27 in Strains Lacking PsbM and PsbT. The possibility that Psb27 may play a role in PSII assembly and repair (*8, 29, 30*) prompted us to investigate the effects of removing Psb27 in the ΔPsbM and ΔPsbT mutants. Figure 7A shows the interruption of *psb27* with a chloramphenicol-resistance cassette in wild type and the ΔPsbM and ΔPsbT mutant backgrounds. The removal of Psb27 in wild type and the ΔPsbT mutant had no effect on photoautotrophic growth; however, photoautotrophic growth was abolished in the ΔPsbM:ΔPsb27 strain (Figure 7B). The ΔPsbM:ΔPsb27 strain was also incapable of oxygen evolution (Figure 7C) or assembly of PSII centers (Figure 7D). In contrast, oxygen evolution and the relative number of assembled PSII centers were similar to wild type in the ΔPsb27 strain. Moreover, when compared to wild type, the ΔPsbT:ΔPsb27 mutant exhibited an oxygen evolution rate of 72% and assembled PSII centers to a level of 48%, which were similar values to those for ΔPsbT cells (Figure 2C, D and Figure 7C, D).

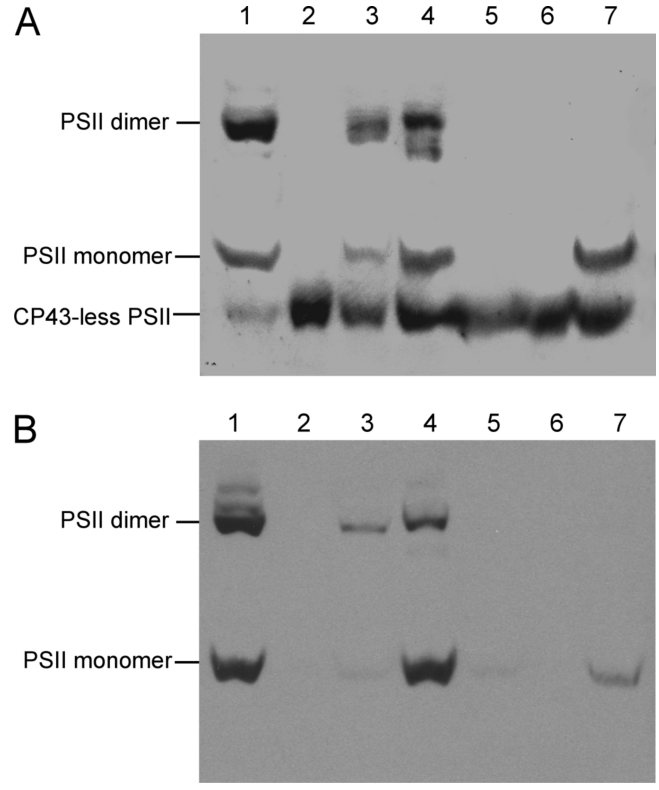

FIGURE 5: Immunodetection of PSII core complexes from thylakoid membranes using (A) D1, and (B) CP43 antibodies following separation by BN−PAGE. Thylakoids were solubilized with 1% *n*-dodecyl β-D-maltoside, and 5 μg of chlorophyll was loaded onto a 5−12% gradient gel. Protein was transferred to PVDF membrane for detection. Lanes: 1, wild type; 2, ΔPsbL; 3, ΔPsbM; 4, ΔPsbT; 5, ΔPsbL:ΔPsbM; 6, ΔPsbL:ΔPsbT; 7, ΔPsbM:ΔPsbT.

In Figure 7E the effect of removing Psb27 on recovery of oxygen evolution following exposure to high-light stress is presented. The ΔPsb27 strain was found to acclimate to the stress condition and exhibited an increased rate of oxygen evolution upon returning to low light as seen with wild type. However, the ΔPsbT:ΔPsb27 strain was unable to recover any oxygen-evolving activity. This is in contrast to the ΔPsbT strain, which exhibited a complete protein-synthesis-dependent recovery under identical conditions (Figure 6A).

Blue-native PAGE was used to determine the composition of PSII monomers and PSII dimers in the strains lacking Psb27. Photosystem II complexes were detected using antibodies to D1 (Figure 8A) and CP43 (Figure 8B). Similar results to Figure 8A were obtained with antibodies to D2 and CP47 (data not shown). The abundance of dimers and monomers in the ΔPsb27 strain was similar to wild type, indicating removal of Psb27, under our experimental conditions, was insufficient to disrupt assembly of PSII. The removal of Psb27 from the ΔPsbT strain also had no apparent effect. The characteristic PSII dimer doublet of the ΔPsbT strain (Figure 5A) was also present in the ΔPsbT:ΔPsb27 mutant, therefore combined removal of Psb27 and PsbT was also insufficient to prevent dimer formation or assembly of PSII monomeric complexes. In contrast, in the ΔPsbM:ΔPsb27 strain, only the CP43-less subcomplex was formed, providing evidence that removal of Psb27 from the ΔPsbM strain arrests PSII biogenesis.

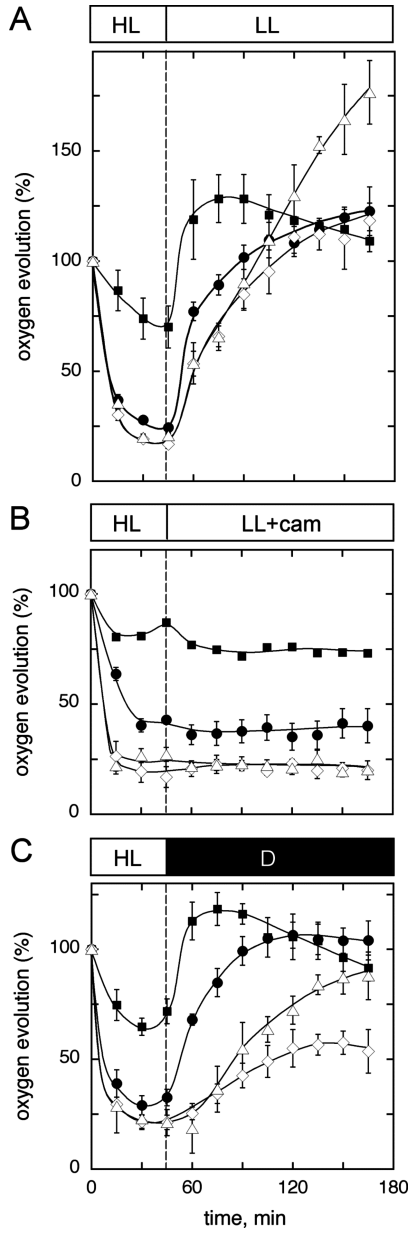

FIGURE 6: Recovery of oxygen-evolving activity following high-light stress. Cell suspensions at 10 μg of chlorophyll/mL were subjected to 45 min of high-intensity white light at 2.0 mE m^{-2} s^{-1} (HL), then allowed to recover under (A) low-light conditions (0.03 mE m^{-2} s^{-1}), (B) low-light conditions in the presence of chloramphenicol (cam) (added at 45 min when light stress removed), and (C) dark. Strains: wild type (closed squares), ΔPsbM (closed circles), ΔPsbT (open diamonds), ΔPsbM:ΔPsbT (open triangles). The data are the average ± the standard error of three independent experiments.

DISCUSSION

Deletion of psbM in Synechocystis sp. PCC 6803. Removal of PsbM in ΔPsbM cells resulted in a 28% reduction of assembled PSII centers, with a concomitant reduction in PSII activity and an increased photoautotrophic doubling time. These results were corroborated by a reduction in both monomer and dimer formation and the appearance of the CP43-less monomer subcomplex. This suggests an important role for PsbM in assembly of active monomeric PSII from the CP43-less assembly intermediate. Disrupted assembly in the ΔPsbM mutant appears to differ from tobacco where PsbM is not required for biogenesis of higher order PSII complexes (*31*). Moreover, recombination of Q_A^- with the S_2 state appeared to be similar in wild type and ΔPsbM cells, whereas in the tobacco Δ*psbM* mutant, backward electron flow was impaired (*31*). Our findings also indicated only a slight alteration in the forward rate between Q_A^- and Q_B, again contrasting with evidence for an altered Q_B binding site in Δ*psbM* tobacco plants (*31*). However, ΔPsbM cells were light sensitive and rapidly photoinactivated, which is consistent with an observed increased light sensitivity in the tobacco mutant.

In our ΔPsbM mutant, recovery from high-light-induced damage proceeded during a dark incubation in a similar fashion to recovery observed in the light. Dark-recovery of photodamaged PSII has been reported in *Synechocystis* sp. PCC 6803 following high-light stress in combination with low temperature which traps PSII in an inactive state (*32*−*34*). We therefore hypothesize that PSII in ΔPsbM cells also enters a dark-reversible inactive state in our experiments. However, further studies are required to verify if the PSII intermediate state identified by Murata and co-workers is related to the inactive state of PSII in ΔPsbM cells.

Inactivation of psbT in Cyanobacteria. The *psbT* gene has been inactivated in *T. elongatus* and did not impair photoautotrophic growth or oxygen evolution. However, a decrease in the number of dimers was obtained following isolation of PSII core complexes and anion exchange chromatography (*7*). In *Synechocystis* sp. PCC 6803, PsbT has 50% identity with PsbT from *T. elongatus*. The majority of sequence similarity is associated with the C-terminal half of the polypeptide and amino acid residue differences in the N-terminal region retain the hydrophobicity contributing to the α helix that spans the membrane (Figure S3 in the Supporting Information).

The ΔPsbT mutant in *Synechocystis* sp. PCC 6803 exhibited slowed photoautotrophic growth, with oxygen evolution 62% of wild type and PSII assembly reduced to a similar extent. This suggests fewer assembled PSII centers in the strain lacking PsbT than in the ΔPsbM mutant. Moreover, ΔPsbT cells showed slowed Q_A^- reoxidation after a single turnover flash in contrast to the situation in the ΔPsbM strain. However, our BN−PAGE data for the ΔPsbT mutant suggest slightly elevated levels of the different PSII complexes than seen in ΔPsbM cells, and it is possible that an altered acceptor side in ΔPsbT cells may have resulted in an underestimation of PSII centers by our herbicide-binding assay. However, the apparent dissociation constant for both ΔPsbM and ΔPsbT cells was ∼380 nM compared to ∼250 nM for wild type.

Results with *T. elongatus* suggested that PsbM may not bind to PSII in the absence of PsbT (*7*); however, in *Synechocystis* sp. PCC 6803 we found the removal of PsbM was additive when combined with the removal of PsbT. The ΔPsbM:ΔPsbT double mutant was found to only have monomeric forms of PSII but retained sufficient active PSII complexes to support photoautotrophic growth, although oxygen evolution was rapidly photoinactivated. There was also an additive effect on forward electron transfer in the double mutant with an increase in the amplitude of the slower component(s) over that observed for the ΔPsbT strain. However, the number of assembled PSII centers detected by our herbicide-binding assay remained similar to the levels observed in the single ΔPsbT mutant.

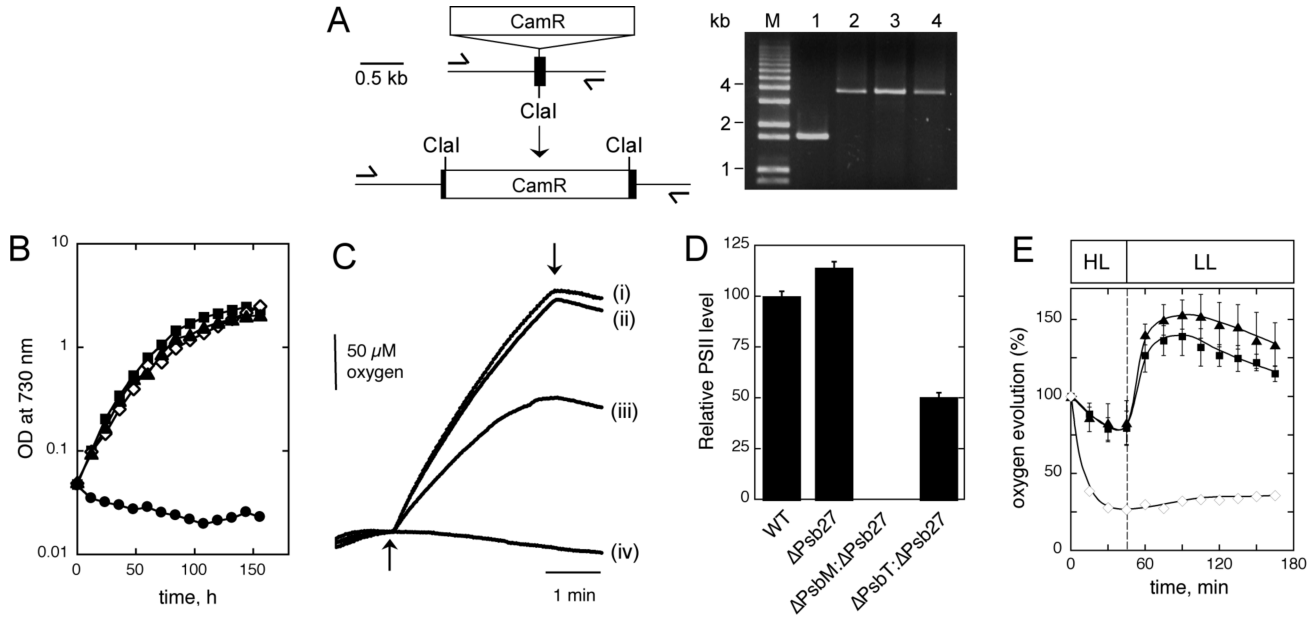

FIGURE 7: The effect of removing Psb27 in wild type and mutant strains. (A) Insertion of a 2.0-kb chloramphenicol-resistance cassette (CamR) within the unique intragenic *Cla*I site of *psb27*. PCR verification of complete segregation of the interrupted *psb27* gene is shown. Lanes: M, 1 Kb Plus DNA Ladder (Invitrogen, Carlsbad, CA); 1, wild type; 2, ΔPsb27; 3, ΔPsbM:ΔPsb27; 4, ΔPsbT:ΔPsb27. (B) Photoautotrophic growth as measured by the optical density at 730 nm. Strains shown are wild type (closed squares), ΔPsb27 (closed triangles), ΔPsbM:ΔPsb27 (closed circles), ΔPsbT:ΔPsb27 (open diamonds). The data are representative of three independent experiments. (C) Traces of oxygen evolution in the presence of $K_3Fe(CN)_6$ and DMBQ. The 1 mL reaction chamber held cell suspensions containing 10 μg of chlorophyll/mL. Average initial rates of oxygen evolution over the first min of illumination are given in μmol of O_2 (mg of chlorophyll)$^{-1}$ h^{-1}. Data are representative of three independent experiments and rates were reproducible to within 15% of the average. (i) Wild type, 483; (ii) ΔPsb27, 473; (iii) ΔPsbT:ΔPsb27, 372; (iv) ΔPsbM:ΔPsb27, no measurable rate. Arrows indicate when light was turned on and off. (D) Relative levels of PSII assembly as determined by DCMU-replaceable [^{14}C]atrazine binding, normalized to a wild-type chlorophyll/PSII ratio of 746. The data are the average ± the standard error of three independent experiments. (E) Recovery of oxygen-evolving activity following high-light stress. Cell suspensions at 10 μg of chlorophyll/mL were subjected to 45 min of high-intensity white light at 2.0 mE m^{-2} s^{-1} (HL), then allowed to recover under low-light conditions (0.03 mE m^{-2} s^{-1}). Strains: wild type (closed squares), ΔPsb27 (closed triangles), ΔPsbT:ΔPsb27 (open diamonds). The data are the average ± the standard error of three independent experiments.

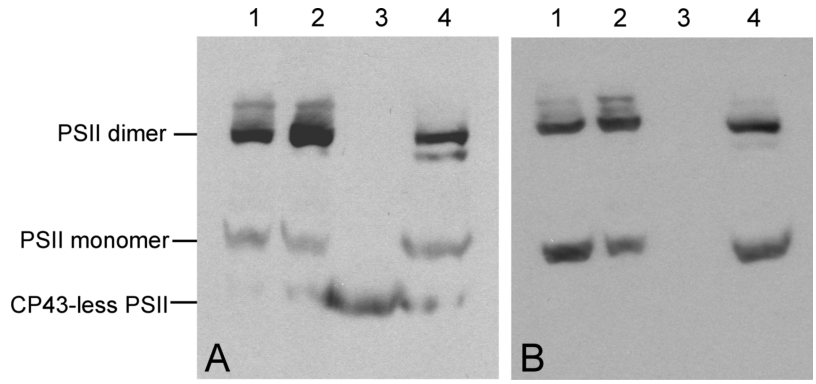

FIGURE 8: Immunodetection of PSII core complexes from thylakoid membranes using (A) D1 and (B) CP43 antibodies following separation by BN−PAGE. Thylakoids were solubilized with 1% *n*-dodecyl β-D-maltoside, and 5 μg of chlorophyll was loaded onto a 5−12% gradient gel. Protein was transferred to PVDF membrane for detection. Lanes: 1, wild type; 2, ΔPsb27; 3, ΔPsbM:ΔPsb27; 4, ΔPsbT:ΔPsb27.

In the green alga *Chlamydomonas reinhardtii*, the rate of photodamage was found to be similar in wild type and ΔPsbT cells (*11, 12*); however, the rate of photodamage or inactivation of PSII activity was accelerated in our ΔPsbT strain when compared to wild type (Figure 6 and ref *35*). Nevertheless, as in *C. reinhardtii*, our ΔPsbT strain exhibited a slower recovery than wild type when the high-light stress was removed. Moreover, in the dark, recovery was incomplete and thus required additional light-dependent steps not required in ΔPsbM cells. Also, recovery of oxygen evolution following inactivation by high light was blocked by both chloramphenicol (Figure 6B) and lincomycin (*35*) in our ΔPsbT strain; whereas the dark recovery in ΔPsbM cells was not prevented when lincomycin was added immediately prior to the recovery phase following high-light treatment (*35*).

Intriguingly, ΔPsbM:ΔPsbT cells recovered to a greater extent than ΔPsbT cells in the dark following high-light exposure and, under low light, recovered to give rates of oxygen evolution considerably higher on a chlorophyll basis than observed before the cells were stressed. Our BN−PAGE conditions failed to detect any dimers in this mutant, suggesting that persistence of monomers in this strain may affect regulation of active PSII levels. However, it is possible dimers formed but were susceptible to the 1% *n*-dodecyl β-D-

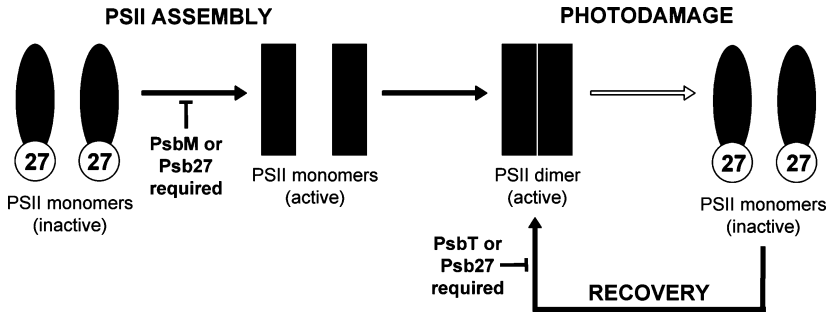

FIGURE 9: Requirement for Psb27 in the ΔPsbM and ΔPsbT mutants. The ΔPsbM strain cannot form active PSII monomers if Psb27 is not present and ΔPsbT cells cannot recover from high-light-induced stress if Psb27 is absent. In the figure Psb27 is shown associated with the inactive monomer (*8*).

maltoside treatment performed prior to electrophoresis, resulting in only monomeric PSII being observed in our experiment.

The Effect of Removing Psb27 in ΔPsbM and ΔPsbT Cells. Although absent from X-ray crystallographic structures of PSII, Psb27, a lumenal polypeptide, has been detected in inactive PSII monomers lacking the PsbO, PsbU and PsbV extrinsic subunits of *T. elongatus* (*8, 29*). Moreover, Psb27 is present in isolated PSII complexes from *Synechocystis* sp. PCC 6803 where it facilitates photoactivation of PSII (*9, 30*). We therefore investigated the requirement for Psb27 in the recovery from high-light stress in the ΔPsbM and ΔPsbT strains. Unexpectedly, the ΔPsbM:ΔPsb27 strain could not assemble PSII centers beyond CP43-less monomers. In contrast, recovery of ΔPsb27 cells was prevented in the ΔPsbT:ΔPsb27 mutant although the phenotype was otherwise similar to the ΔPsbT strain. These data are summarized in Figure 9 and demonstrate that the absence of Psb27 introduced a complete block in biogenesis in the ΔPsbM background but selectively blocked the recovery process in cells lacking PsbT.

The Requirement for PsbL in Cyanobacterial Photosystem II. In contrast to an earlier report with a *psbL* deletion mutant of *Synechocystis* sp. PCC 6803 where no photoautotrophic growth was observed (*10*), we found removal of PsbL resulted in limited photoautotrophic growth with a doubling time of >120 h. Given this difference we verified the absence of PsbL in our mutant using a PsbL-specific antibody (Figure S4 in the Supporting Information). We have also recently constructed a *psbL* deletion mutant and found there was no message expressed for *psbJ*; however, we did obtain message for *psbJ* in our interruption mutant indicating that PsbJ may be present in our ΔPsbL strain (Figure S5 in the Supporting Information). Hence our results indicate the obligate photoheterotrophic phenotype associated with deletion of *psbL* in *Synechocystis* sp. PCC 6803 arises from the concomitant inactivation of *psbJ*. However, limited photoautotrophic growth is still possible when *psbL* has been interrupted provided *psbJ* expression is not prevented.

The Effect of High-Light Exposure on Oxygen Evolution in Wild Type. For this study experimental conditions were selected whereby the rate of photodamage and repair were balanced in wild-type cells (Figure S6 in the Supporting Information). We observed an initial drop to approximately 75% of the initial rate following an ~45 min exposure to 2 mE m^{-2} s^{-1} at 30 °C at a chlorophyll concentration of 10 μg/mL. When these conditions continued over 2 h, the cells were subsequently able to acclimate with oxygen evolution recovering to ~90% of the initial rate (*35*). These experiments led to the discovery that a pre-exposure to high light induced oxygen evolution in wild-type cells to ~125% of their initial activity when transferred back to low light (0.3 mE m^{-2} s^{-1}). In Figure 6B we demonstrate that this effect requires protein synthesis and is abolished by the addition of chloramphenicol.

Interestingly, we have recently reported that the observed stimulation of oxygen evolution when transferring cells from our high-light to low-light conditions is insensitive to lincomycin (*35*). It is known that high light exposure results in elevated association of *psbA* mRNA with polysomes (*36*) and that lincomycin does not interact with ribosomes with bound nascent peptides and will therefore not act on preformed polysomes. However, chloramphenicol is effective against peptide bond formation in ribosomes and polysomes (*37*). Therefore our working hypothesis is that additional stimulation of oxygen evolution upon transferring cells to low-light conditions arises from the insertion of preformed D1 from membrane-associated polysomes. Our results also suggest that this incorporation of newly synthesized D1 does not require light (Figure 6C). Moreover, this phenomenon is observed in cells lacking PsbM but does not occur in ΔPsbT cells.

ACKNOWLEDGMENT

Dr. Fiona Bentley acknowledges travel support to visit Oklahoma State University provided by the Marjorie McCallum fund at the University of Otago.

SUPPORTING INFORMATION AVAILABLE

Table S1 analyzing the distribution of the S-states from Figure 4A; amino acid sequence alignments for PsbL, PsbM and PsbT; immunodetection of PsbL in isolated thylakoid membranes from wild type and the ΔPsbL strain; reverse transcriptase PCR of *psbE*, *psbF*, *psbL* and *psbJ* in wild type, a *psbL* deletion mutant and the *psbL* interruption strain; and a time course of photoinactivation as measured by oxygen evolution for the ΔPsbM and ΔPsbT strains. This material is available free of charge via the Internet at http://pubs.acs.org.

REFERENCES

1. Williams, J. G. K. (1988) Construction of specific mutations in photosystem II photosynthetic reaction center by genetic engineering methods in *Synechocystis* 6803. *Methods Enzymol. 167*, 766–778.

2. Vermaas, W. F. J. (1998) Gene modifications and mutation mapping to study the function of photosystem II. *Methods Enzymol. 297*, 293–311.
3. Ikeuchi, M., and Tabata, S. (2001) *Synechocystis* sp. PCC 6803 a useful tool in the study of the genetics of cyanobacteria. *Photosynth. Res. 70*, 73–83.
4. Ferreira, K. N., Iverson, T. M., Maghlaoui, K., Barber, J., and Iwata, S. (2004) Architecture of the photosynthetic oxygen-evolving center. *Science 303*, 1831–1838.
5. Loll, B., Kern, J., Saenger, W., Zouni, A., and Biesiadka, J. (2005) Towards complete cofactor arrangement in the 3.0 Å resolution structure of photosystem II. *Nature 438*, 1040–1044.
6. Kawakami, K., Iwai, M., Ikeuchi, M., Kamiya, N., and Shen, J.-R. (2007) Location of PsbY in oxygen-evolving photosystem II revealed by mutagenesis and X-ray crystallography. *FEBS Lett. 581*, 4983–4987.
7. Iwai, M., Katoh, H., Katayama, M., and Ikeuchi, M. (2004) PSII-Tc protein plays an important role in dimerization of photosystem II. *Plant Cell Physiol. 45*, 1809–1816.
8. Nowaczyk, M. M., Hebeler, R., Schlodder, E., Meyer, H. E., Warscheid, B., and Rögner, M. (2006) Psb27, a cyanobacterial lipoprotein, is involved in the repair cycle of Photosystem II. *Plant Cell 18*, 3121–3131.
9. Kashino, Y., Lauber, W. M., Carroll, J. A., Wang, Q., Whitmarsh, J., Satoh, K., and Pakrasi, H. B. (2002) Proteomic analysis of a highly active photosystem II preparation from the cyanobacterium *Synechocystis* sp. PCC 6803 reveals the presence of novel polypeptides. *Biochemistry 41*, 8004–8012.
10. Anbudurai, P. R., and Pakrasi, H. B. (1993) Mutational analysis of the PsbL protein of photosystem II in the cyanobacterium *Synechocystis* sp. PCC 6803. *Z. Naturforsch. 48*, 267–274.
11. Ohnishi, N., and Takahashi, Y. (2001) PsbT polypeptide is required for efficient repair of photodamaged photosystem II reaction center. *J. Biol. Chem. 276*, 33798–33804.
12. Ohnishi, N., Kashino, Y., Satoh, K., Ozawa, S., and Takahashi, Y. (2007) Chloroplast-encoded polypeptide PsbT is involved in the repair of primary electron acceptor Q_A of photosystem II during photoinhibition in *Chlamydomonas reinhardtii*. *J. Biol. Chem. 283*, 7107–7115.
13. Eaton-Rye, J. J. (2004) The construction of gene knockouts in the cyanobacterium *Synechocystis* sp. PCC 6803, in *Methods of Molecular Biology, Vol 274: Photosynthesis Research Protocols* (Carpentier, R., Ed.) pp 309−324, Humana Press, Totowa, NJ.
14. Summerfield, T. C., Shand, J. A., Bentley, F. K., and Eaton-Rye, J. J. (2005) PsbQ (Sll1638) in *Synechocystis* sp. PCC 6803 is required for photosystem II activity in specific mutants and in nutrient-limiting conditions. *Biochemistry 44*, 805–815.
15. Boliver, F. (1978) Construction and characterization of new cloning vehicles, III. Derivatives of plasmid pBR322 carrying unique EcoRI sites for selection of EcoRI-generated recombinant DNA molecules. *Gene 4*, 121–126.
16. Prentki, P., Karch, F., Iida, S., and Meyer, J. (1981) The plasmid cloning vector pBR325 contains a 482 base-pair-long inverted duplication. *Gene 14*, 289–299.
17. Elhai, J., and Wolk, C. P. (1988) A versatile class of positive-selection vectors based on the nonviability of palindrome-containing plasmids that allows cloning into long polylinkers. *Gene 68*, 119–138.
18. Prentki, P., and Krisch, H. M. (1984) In vitro insertional mutagenesis with a selectable DNA fragment. *Gene 29*, 303–313.
19. Vermaas, W. F. J., Charité, J., and Shen, G. (1990) Q_A binding to D2 contributes to the functional and structural integrity of photosystem II. *Z. Naturforsch. 45C*, 359–365.
20. Morgan, T. R., Shand, J. A., Clarke, S. M., and Eaton-Rye, J. J. (1998) Specific requirements for cytochrome *c*-550 and the manganese-stabilizing protein in photoautotrophic strains of *Synechocystis* sp. PCC 6803 with mutations in the domain Gly-351 to Thr-436 of the chlorophyll-binding protein CP47. *Biochemistry 37*, 14437–14449.
21. Burnap, R. L., Qian, M., and Pierce, C. (1996) The manganese-stabilizing protein of photosystem II modifies the in vivo deactivation and photoactivation kinetics of the H_2O oxidation complex in *Synechocystis* sp. PCC6803. *Biochemistry 35*, 874–882.
22. MacKinney, G. (1941) Absorption of light by chlorophyll solutions. *J. Biol. Chem. 140*, 315–322.
23. Kügler, M., Jänsch, L., Kruft, V., Schmitz, U. K., and Braun, H.-P. (1997) Analysis of the chloroplast protein complexes by blue-native polyacrylamide gel electrophoresis (BN-PAGE). *Photosynth. Res. 53*, 35–44.
24. Rokka, A., Suorsa, M., Saleem, A., Battchikova, N., and Aro, E.-M. (2005) Synthesis and assembly of thylakoid protein complexes: multiple assembly steps of photosystem II. *Biochem. J. 388*, 159–168.
25. Whitehead, T. P., Kricka, L. J., Carter, T. J. N., and Thorpe, G. H. G. (1979) Analytical luminescence: Its potential in the clinical laboratory. *Clin. Chem. 25*, 1531–1546.
26. Vass, I., Kirilovsky, D., and Etienne, A.-L. (1999) UV-B radiation-induced donor- and acceptor-side modifications of photosystem II in the cyanobacterium *Synechocystis* sp. PCC 6803. *Biochemistry 38*, 12786–12794.
27. Komenda, J., Reisinger, V., Müller, B. C., Dobáková, M., Granvogl, B., and Eichacker, L. A. (2004) Accumulation of the D2 protein is a key regulatory step for assembly of the photosystem II reaction center complex in *Synechocystis* PCC 6803. *J. Biol. Chem. 279*, 48620–48629.
28. Suorsa, M., Regel, R. E., Paakkarinen, V., Battchikova, N., Herrmann, R. G., and Aro, E.-M. (2004) Protein assembly of photosystem II and accumulation of subcomplexes in the absence of low molecular mass subunits PsbL and PsbJ. *Eur. J. Biochem. 271*, 96–107.
29. Mamedov, F., Nowaczyk, M. M., Thapper, A., Rögner, M., and Styring, S. (2007) Functional characterization of monomeric photosystem II core preparations from *Thermosynechococcus elongatus* with or without the Psb27 subunit. *Biochemistry 46*, 5542–5551.
30. Roose, J. L., and Pakrasi, H. B. (2008) The Psb27 protein facilitates manganese cluster assembly in photosystem II. *J. Biol. Chem. 283*, 4044–4050.
31. Umate, P., Schwenkert, S., Karbat, I., Dal Bosco, C., Mlcochová, L., Volz, S., Zer, H., Herrmann, R. G., Ohad, I., and Meurer, J. (2007) Deletion of PsbM in tobacco alters the Q_B site properties and electron flow within photosystem II. *J. Biol. Chem. 282*, 9758–9767.
32. Gombos, Z., Wada, H., and Murata, N. (1994) The recovery of photosynthesis from low-temperature photoinhibition is accelerated by the unsaturation of membrane lipids: A mechanism of chilling tolerance. *Proc. Natl. Acad. Sci. U.S.A. 91*, 8787–8791.
33. Allakhverdiev, S. I., Mohanty, P., and Murata, N. (2003) Dissection of photodamage at low temperature and repair in darkness suggests the existence of an intermediate form of photodamaged photosystem II. *Biochemistry 42*, 14277–14283.
34. Mohanty, P., Allakhverdiev, S. I., and Murata, N. (2007) Application of low temperatures during photoinhibition allows characterization of individual steps in photodamage and repair of photosystem II. *Photosynth. Res. 94*, 217–224.
35. Bentley, F. K., and Eaton-Rye, J. J. (2008) The effect of protein synthesis inhibitors on recovery of photodamaged photosystem II in *Synechocystis* sp. PCC 6803 lacking PsbM or PsbT, in *Photosynthesis: Energy from the Sun* (Allen, J. F. , Osmond, B. , Golbeck, J. H., and Gantt, E., Eds.) pp 715−718, Springer, Heidelberg.
36. Tyystjärvi, T., Herranen, M., and Aro, E.-M. (2001) Regulation of translation elongation in cyanobacteria: membrane targeting of the ribosome nascent-chain complexes controls the synthesis of D1 protein. *Mol. Microbiol. 40*, 476–484.
37. Contreras, A., and Vázquez, D. (1977) Cooperative and antagonistic interactions of peptidyl-tRNA and antibiotics with bacterial ribosomes. *Eur. J. Biochem. 74*, 539–547.

BI800804H